Enhanced Power Generation of Airborne Wind Energy System by Foldable Aircraft

Myungjin Jung *, Qiji Ze †, Kai Chuen Tan ‡ Chaoying Pei § Ruike Zhao ¶ Ran Dai ‖
The Ohio State University, Columbus, Ohio, 43210

This paper introduces a novel approach for improving efficiency during the entire generation cycle, especially during the recovery phase by changing the glider's wing configuration. This research presents a virtual efficient model and trajectory to find optimal control problems during the recovery phase. For a glider, we modeled with a common RC glider flight characteristics including power consumption features. The ground part consists of two parts; one is a winch, which follows the dynamics of the ground system's mechanical components. Another is a motor/generator system that portraits the electric performance of a DC machine. An optimal control problem is needed to determine minimum control effort within a designated time objective. The net energy gain improved by morphing the shape during the recovery phase is verified by comparing the simulation results using two models; one is the general glider shape model; another is the folded wing model.

Nomenclature

ρ	=	the atmosphere density, kg/m^3
γ	=	relative flight path angle, deg
ϑ	=	the zenith angle of a glider, deg
φ	=	the azimuth angle of a glider, deg
C_L	=	the aerodynamic lift coefficient
C_D	=	the aerodynamic drag coefficient
D	=	drag force, N
F_t	=	traction force, N
I_{w}	=	moment of inertia of a winch, kgm^2
W	=	the weight of a glider, N
L	=	lift force, N
T	=	thrust of a glider, N
m	=	the mass of a glider, kg
r_{w}	=	radius of a winch, m
S_f	=	the wing area of a folded glider, m^2
S_u	=	the wing area of an unfolded glider, m^2
V	=	velocity of the glider, m/s
$\mathbf{V_w}$	=	velocity of horizontal wind, m/s
$\mathbf{G}$	=	the tether force in navigation frame, N
$\mathbf{P}$	=	the position vector of a glider in navigation frame, m
$\mathbf{V}$	=	the velocity vector of a glider in navigation frame, m/s
α	=	angle of attack of a glider, deg
α_{w}	=	angular acceleration of a winch, rad/s^2
ϕ	=	bank angle of a glider, deg
ψ	=	heading angle of a glider, deg

*Graduate Research Assistant, Mechanical and Aerospace Engineering Department. jung.661@osu.edu
†Postdoctoral Research Fellow , Mechanical and Aerospace Engineering Department. ze.3@osu.edu
‡Undergraduate Research Assistant, Mechanical and Aerospace Engineering Department. tan.783@osu.edu
§Graduate Research Assistant, Mechanical and Aerospace Engineering Department. pei.145@osu.edu
¶Assistant Professor, Mechanical and Aerospace Engineering Department. zhao.2885@osu.edu
‖Assistant Professor, Mechanical and Aerospace Engineering Department. Senior Member AIAA. dai.490@osu.edu

M_c = coulomb friction moment, Nm
M_{gen} = generator torque, Nm

I. Introduction

Wind energy is getting attraction as one of the prominent renewable energy that has achieved $540GW$ cumulative installed power worldwide by the end of 2017 and keeps an increasing trend of gaining an extra $50GW$ every year [1]. A significant number of efforts have focused on constructing taller towers for conventional ground-based wind turbines to take advantage of higher speed and steadier wind at a high altitude. Due to its higher construction cost and environmental constraints, the amount of power generation and flexibility have significantly limited. To overcome such limitations, the airborne wind energy system (AWES) was proposed in the 1980s with capability of harvesting wind energy at significantly increased altitudes around $300m$-$5km$ from the ground surface, which increases the average wind speed from $10m/s$ to $30m/s$ compared with conventional ground-based wind generators [2].

The Ground-Gen AWES, one of the common mechanisms of AWESs, converts mechanical energy into electrical energy by pulling the tethered wire connected to the ground. On account of its low cost for construction, high mobility, and easy operation, this mechanism has attracted increasing attention from both research institutes and industries. One energy production cycle of the Ground-Gen AWES is composed of a generation phase and a recovery phase. In the generation phase, traction force from a kite tethered to the generator unwinds the tether that makes a rotational motion for a generator to produce energy. In the recovery phase, on the other hand, the generator changes its roll to a motor to rewind the tether and pull the kite to the starting location for the next generation phase [3, 4]. Thus far, research has been conducted for developing attitude control or trajectories during the generation phase, which usually accounts for 60 % of the entire production cycle[5–9]. However, the rest of 40 % of period, not only the energy to pull the kite back, but a certain amount of period is required that decreases net energy gain and efficiency during the generation phase. Therefore, novel approaches are required to meet current challenges in increasing the efficiency of AWES.

During the recovery phase, the majority of forces applied to the kite is an aerodynamic force that impedes the rewinding motion. Unlike a fixed body, morphing shape during the recovery phase provides different aerodynamic characteristics that benefit from shortening the length of the period and reducing power consumption from the motor part. Unlike a kite, a fixed-wing aircraft has a propulsion system to provide additional velocity to a body. In order to change the attitude of a kite, tether control [10] is used to change its bank or angle of attack. In addition, there is some research for modeling the kite as a soft and inflatable body on the spherical coordinate system [11, 12]. Also, there are several studies that multi-body [13, 14] dynamics are considered. These approaches cannot neglect the fluid-structure interaction that requires highly sophisticated modeling. On the other hand, the glider platform was chosen for this study because rigid-wing aircraft are well understood and relatively easily modeled compared to soft and flexible bodies such as kites. [15, 16] demonstrates the AWES system based on the unmanned aerial vehicle (UAV) system derived from lagrangian and [17] discusses the 6 degree-of-freedom UAV model with principles of flight dynamics. Moreover, the thrust gives more flexibility to change its attitude or velocity; then, this will benefit from reducing both duration and power consumption from the motor.

As glider needs the energy to control its actuators, the optimal control requires to achieve the entire efficiency improvement. There are several control strategies for AWES, such as figure-eight trajectory [9]; however, the research on the optimal path for the recovering phase named a few. Model predictive control is utilized [18] both generation and recovery phases. In this study, we developed an optimal control scheme to a morphed body that has reduced wind resistance that approaches the generation phase location faster. Eventually, the reduced time occupation and energy consumption of the recovery phase lead to enhances the efficiency of power generation.

The organization of this paper is as follows. §II introduces the entire model consists of a glider, winch, and generator or motor. §III presents the formulation of multi-phase optimal control problem. In §IV, the integrated model for simulation is presented. This result is compared to a nominal glider model. Conclusion is addressed in §V.

II. System Model

In this section, the kinematics and flight dynamics of the entire system are presented. Since the actual model of the mechanical and electric system is nonlinear, a point-mass model for a glider is used. And a linearized model for generator and motor is to the simplified model.

A. Reference Frame

An appropriate coordinate system must be selected to represent a maneuver of an object in space. The inertial coordinate system should be an absolute coordinate system, but it is difficult to define a perfect absolute coordinate system. Also, for a simulation of an aircraft maneuver in the atmosphere, the effect of the earth spinning is negligible. Therefore, the inertial coordinate system can be set on the surface of the earth. In this sense, the inertial coordinate system can be defined as a coordinate system that performs constant velocity motion with respect to the absolute coordinate system.

Assuming AWES generate wind energy near to the surface, then we can consider a flat Earth as reference frame $\boldsymbol{E}$ with its components pointing to east direction as $\hat{\mathbf{e}}_1$, aligned to the north as $\hat{\mathbf{e}}_2$, and the $\hat{\mathbf{e}}_3$ axis points up from the surface. The frame has an origin at the center of gravity of the glider called navigation frame $\boldsymbol{N}$, known as NED frame, $\hat{\mathbf{n}}_1$ axis points north, $\hat{\mathbf{n}}_2$ faces to east, and the $\hat{\mathbf{n}}_3$ axis is facing downward to the surface and this frame also an inertial frame. Assuming a glider as a point mass, we can also express to a non-inertial, rotating reference frame $\boldsymbol{C}$, in this frame the forces acting on the glider are most easily expressed. There is a similar frame called body frame $\boldsymbol{B}$, the origin is at the center of gravity of the glider and is aligned with the roll ϕ, pitch θ, and yaw ψ axis of the aircraft. As $\boldsymbol{C}$ frame, the axis is aligned to the velocity, we use flight path angle γ instead of θ. The $\hat{\mathbf{b}}_1$ axis faces the nose of the glider, the $\hat{\mathbf{b}}_2$ axis points to the right-wing, and $\hat{\mathbf{b}}_3$ axis points down. The stability frame $\boldsymbol{S}$ has an origin fixed at the center of gravity of the glider. The frame rotated by the angle of attack around the $\hat{\mathbf{b}}_2$ axis in the body frame.

The relation between from a navigation frame to $\boldsymbol{C}$ frame is expressed as below,

$$
\begin{aligned}
C_{CN} &= [C_1(\phi)]\,[C_2(\gamma)]\,[C_3(\psi)] \\
&= \begin{bmatrix} 1 & 0 & 0 \\ 0 & \cos\phi & \sin\phi \\ 0 & -\sin\phi & \cos\phi \end{bmatrix} \begin{bmatrix} \cos\gamma & 0 & -\sin\gamma \\ 0 & 1 & 0 \\ \sin\gamma & 0 & \cos\gamma \end{bmatrix} \begin{bmatrix} \cos\psi & \sin\psi & 0 \\ -\sin\psi & \cos\psi & 0 \\ 0 & 0 & 1 \end{bmatrix} \\
&= \begin{bmatrix} \cos\gamma\cos\psi & \cos\gamma\sin\psi & -\sin\gamma \\ -\cos\phi\sin\psi + \sin\phi\sin\gamma\cos\psi & \cos\phi\cos\psi + \sin\phi\sin\gamma\sin\psi & \sin\phi\cos\gamma \\ \sin\phi\sin\psi + \cos\phi\sin\gamma\cos\psi & -\sin\phi\cos\psi + \cos\phi\sin\gamma\sin\psi & \cos\phi\cos\gamma \end{bmatrix}
\end{aligned} \tag{1}
$$

B. Glider Model

Under the point mass assumption, the equation of motion can be derived from $\boldsymbol{C}$ frame, which aligned to the velocity of the glider into the inertial frame. Based on the relationship of two coordinate systems, The position of the glider expressed in a navigation frame is given as follows,

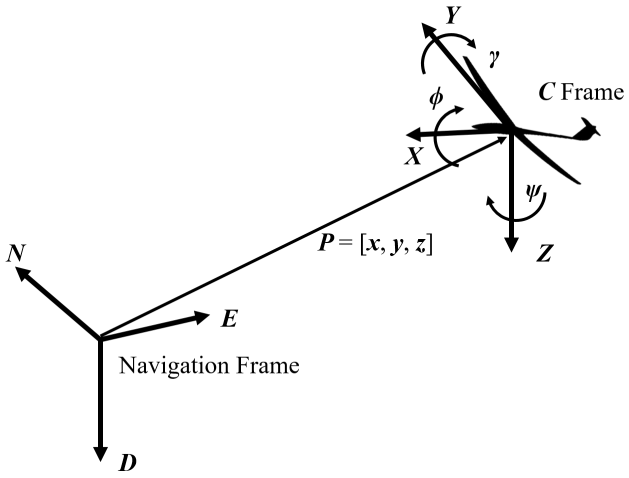

Fig. 1 Transform of the frames

$$
\mathbf{P} = x\hat{\mathbf{n}}_1 + y\hat{\mathbf{n}}_2 + z\hat{\mathbf{n}}_3 \tag{2}
$$

The velocity of the glider can be shown in the navigation frame, and $\boldsymbol{C}$ frame is written as below,

$$\mathbf{V} = \dot{\mathbf{P}} = \dot{x}\hat{\mathbf{n}}_1 + \dot{y}\hat{\mathbf{n}}_2 + \dot{z}\hat{\mathbf{n}}_3 = V\hat{\mathbf{c}}_1 \tag{3}$$

The equation of motion can be derived by using Newton's law and transport theorem; it is represented in $\boldsymbol{C}$ frame.

$$\frac{d}{dt}\mathbf{V}^N = \frac{d}{dt}\mathbf{V}^C + \omega_{NC} \times \mathbf{V} \tag{4}$$

Then, we can derive acceleration in navigation frame,

$$\dot{\mathbf{V}} = \dot{V}\hat{\mathbf{c}}_1 + V\left(-\dot{\gamma}\sin\phi + \dot{\psi}\cos\gamma\cos\phi\right)\hat{\mathbf{c}}_2 - V\left(\dot{\gamma}\cos\phi + \dot{\psi}\cos\gamma\sin\phi\right)\hat{\mathbf{c}}_3 \tag{5}$$

In the same sense, we can elaborate the velocity in $\boldsymbol{C}$ to $\boldsymbol{N}$ by using transformation matrix, $[C_{CN}]^T$. Then the inertial velocity of the glider is shown as

$$\mathbf{V} = V\cos\gamma\cos\psi\hat{\mathbf{n}}_1 + V\cos\gamma\sin\psi\hat{\mathbf{n}}_2 - V\sin\gamma\hat{\mathbf{n}}_3 \tag{6}$$

Fig. 2 shows a free body diagram of the point mass glider. Multiple external forces are acting on the glider body, lift force L, thrust T, tether force from generator G, weight W, and drag force D. As we define the body frame, the $\hat{\mathbf{c}}_1$ axis is aligned with thrust, $\hat{\mathbf{c}}_2$ axis is faces to the right-wing, and $\hat{\mathbf{c}}_3$ axis has opposite direction with lift force, and direction of weight is in $\hat{\mathbf{n}}_3$ axis direction. However, we cannot define the direction of tether force from the generator, as tension can be applied from the arbitrary direction from the bottom of the glider, so we define tension in $\boldsymbol{C}$ frame as G_{xc}, G_{yc}, and G_{zc} respectively. Then using transformation matrix defined above, the tether force acting on $\boldsymbol{C}$ frame can be written as

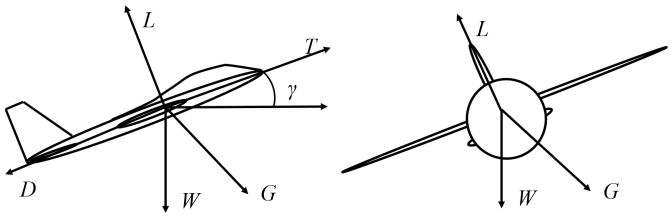

Fig. 2 Free body diagram of the glider

$$\begin{bmatrix} G_{xc} \\ G_{yc} \\ G_{zc} \end{bmatrix} = \begin{bmatrix} \cos\gamma\cos\psi & \cos\gamma\sin\psi & -\sin\gamma \\ -\cos\phi\sin\psi + \sin\phi\sin\gamma\cos\psi & \cos\phi\cos\psi + \sin\phi\sin\gamma\sin\psi & \sin\phi\cos\gamma \\ \sin\phi\sin\psi + \cos\phi\sin\gamma\cos\psi & -\sin\phi\cos\psi + \cos\phi\sin\gamma\sin\psi & \cos\phi\cos\gamma \end{bmatrix} \begin{bmatrix} G_x \\ G_y \\ G_z \end{bmatrix} \tag{7}$$

$$\begin{aligned} G_x &= -\mathbf{G}\sin\vartheta\cos\varphi \\ G_y &= -\mathbf{G}\sin\vartheta\sin\varphi \\ G_z &= -\mathbf{G}\cos\vartheta \\ \vartheta &= \arctan(\frac{y}{x}) \\ \varphi &= \arccos(\frac{z}{d}) \\ d &= \sqrt{x^2 + y^2 + z^2} \end{aligned} \tag{8}$$

where ϑ is the azimuth angle of a glider, φ is the zenith angle of a glider, $\mathbf{G}$ is a magnitude of tether force to a glider, and d is the distance between the winch and the glider. Then, as shown in Fig. 2, the dynamic equations expressed in $\boldsymbol{C}$ frame, by using equation (5) then,

$$\begin{aligned} m\dot{V} &= T - D - W\sin\gamma + G_{xc} \\ mV\left(-\dot{\gamma}\sin\phi + \dot{\psi}\cos\gamma\cos\phi\right) &= W\cos\gamma\sin\phi + G_{yc} \\ -mV\left(\dot{\gamma}\cos\phi + \dot{\psi}\cos\gamma\sin\phi\right) &= -L + W\cos\gamma\cos\phi + G_{zc} \end{aligned} \tag{9}$$

To summarize, the equations of motion of the glider as ordinary differential equation forms are shown below,

$$\begin{aligned}
\dot{x} &= V\cos\gamma\cos\psi \\
\dot{y} &= V\cos\gamma\sin\psi \\
\dot{z} &= -V\sin\gamma \\
\dot{V} &= \frac{T - D + G_{xc}}{m} + g\sin\gamma \\
\dot{\gamma} &= \frac{L\cos\phi - G_{yc}\sin\phi - G_{zc}\cos\phi}{mV} - \frac{g\cos\gamma}{V} \\
\dot{\psi} &= \frac{L\sin\phi + G_{yc}\cos\phi - G_{zc}\sin\phi}{mV\cos\gamma}
\end{aligned} \tag{10}$$

In this paper, wind effect is also important to affect the maneuver of a glider. In this paper, we assume that there is only horizontal wind, and wind shear does not exist. Then, we need to consider wind to provide relative wind velocity to the glider. Suppose there is horizontal wind V_w expressed in the navigation frame.

$$\mathbf{V_w} = V_{wx}\hat{\mathbf{n}}_1 + V_{wy}\hat{\mathbf{n}}_2 \tag{11}$$

Then, inertial velocity combined to the velocity of the glider (6) and the velocity of the wind (11) represented in navigation frame can be written as

$$V = (V\cos\gamma\cos\psi + V_{wx})\,\hat{\mathbf{n}}_1 + \left(V\cos\gamma\sin\psi + V_{wy}\right)\hat{\mathbf{n}}_2 - V\sin\gamma\hat{\mathbf{n}}_3 \tag{12}$$

The actual wind speed and direction vary by time and location. Then, the velocity of horizontal wind $V_w x$, $V_w y$ are the functions of time, x, y, and z[19]. Assuming constant wind $\left(\frac{\partial V_{wx}}{\partial t} = \frac{\partial V_{wy}}{\partial t} = \frac{\partial V_{wz}}{\partial t} \approx 0\right)$, and equations (12) applied to the derivatives of γ and ψ then we can get the equation of motion of glider with the wind as ODE form as written as below;

$$\begin{aligned}
\dot{x} &= V\cos\gamma\cos\psi + V_{wx} \\
\dot{y} &= V\cos\gamma\sin\psi + V_{wy} \\
\dot{z} &= -V\sin\gamma \\
\dot{V} &= \frac{T - D + G_{xc}}{m} - g\sin\gamma \\
\dot{\gamma} &= \frac{L\cos\phi - G_{yc}\sin\phi - G_{zc}\cos\phi}{mV} - \frac{g\cos\gamma}{V} \\
\dot{\psi} &= \frac{L\sin\phi + G_{yc}\cos\phi - G_{zc}\sin\phi}{mV\cos\gamma}
\end{aligned} \tag{13}$$

C. Winch and DC Machine Model

The winch was designed and built for the interconnection between a DC machine and a glider. During the generation phase, this model converts the traction force to the rotational motion of the generator. For the recovery phase, rotational motion from the motor rewinds the unwound cable to prepare for the next energy generation phase. Based on the relationship, the dynamic model of the winch can be formulated as below

$$I_{\mathrm{w}}\alpha_{\mathrm{w}} = r_{\mathrm{w}}F_t - M_{\mathrm{c}} - M_{\mathrm{gen}} \tag{14}$$

where I_{w} is the moment of inertia of a winch, α_{w} is angular acceleration of a winch, r_{w} is radius of a winch, F_t is the traction force, M_{c} is coulomb friction moment, M_{gen} is the torque of the DC machine.

Considering the AWES have two working phases, a generator and a motor are needed to be used for energy generation in the generation phase and retrieving the glider back in the recovery phase. We utilized the integrated motor/generator technology to adopt a permanent magnet DC machine work as generator and motor simultaneously by using an asymmetric half-bridge power converter shown in Fig. 3 to change the working modes.

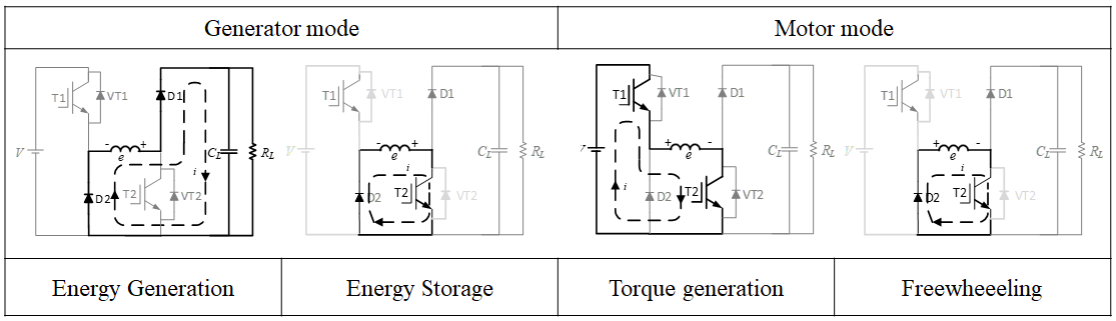

Fig. 3 Function of half-bridge

In the generation phase, the DC machine works in the generator mode and has two working stages, namely energy generation and energy storage as shown in Fig. 3 by controlling the switch T2. When the switch is turned off, the current flows through two diodes and is governed by the equations:

$$\begin{aligned} e &= u_L + Ri + L_a \frac{di}{dt} + 2U_d \\ i &= \frac{u_L}{R_L} + C_{\text{Link}} \frac{du_L}{dt} \end{aligned} \tag{15}$$

where e is the counter-electromotive force (CEMF) of the armature winding, u_L is the voltage of the load side, R is the armature resistance, L_a is the armature inductance, U_d is the voltage drop of the diode and switch, R_L is the load resistance, C_{Link} is the DC-link capacitor, and i is the armature current, which will also determine the electromagnetic torque T_e of the machine and the dynamic motion of the machine is governed by the kinematic equation:

$$\begin{aligned} T_e &= K_t i \\ J\frac{d\omega}{dt} &= T_e - T_L - B_m\omega - T_f \\ e &= K_e\omega \end{aligned} \tag{16}$$

where J is the moment of inertia of the rotor, T_L is the load torque from the glider, B_m is the viscous friction coefficient, T_f is the Coulomb friction torque, and ω is the rotation speed of the machine, which also determine the CEMF, and K_e is the voltage constant of the machine. In addition, it should be noted that T_e and T_L have different signs in the generation mode and motor mode and follow these principles:

$$\begin{aligned} &\text{if } T_e, T_L < 0 : \text{generator mode} \\ &\text{if } T_e, T_L > 0 : \text{motor mode} \end{aligned} \tag{17}$$

In contrast, when the switch T2 is turned on, the current flows through diode D2 and switch T2 and follows the voltage equation:

$$e = Ri + L_a \frac{di}{dt} + 2U_d \tag{18}$$

In this case, the current will increase as the CEMF have the same direction as the armature current. And it generally increases the power generation capability by increase the electromagnetic torque. In this paper, considering we apply the optimal trajectory of the glider to obtain the maximum energy generation, the converter in the generator mode will be a passive rectifier. The generator will only work on the energy generation stage to simplify the control strategy. However, we can also apply the maximum power point tracking algorithm on the generator side to improve the net energy generation.

In the retrieving phase, the DC machine works in the motor mode and has two working stages, namely torque generation and freewheeling, as shown in Fig. 3by controlling the switches T1 and T2. When both switches are turned on, the current flows through two switches and is governed by the armature voltage equation:

$$V_a = e + Ri + L_a \frac{di}{dt} + 2U_d \tag{19}$$

Where V_a is the voltage of the DC power source. In contrast, when only switch T2 is turned on, the current cannot sudden decrease to zero and will freewheel through diode D2. In this case, the current will decrease as the CEMF have the opposite direction with the armature current. And it generally decreases the output torque. By using a PI controller, the duty cycle of the switch T1 can be controlled based on the feedback of motor speed to achieve constant speed control. To achieve the maximum net generation efficiency, a maximum efficiency point tracking algorithm can also be applied in the motor side to find a balance between energy consumption and retrieving time.

III. Optimal Control Problem

While generating electricity from the ground generator, the glider also consumes energy due to the thrust. Therefore, the amount of energy produced from the generator should larger than the amount of energy for the propulsion and rewinding motion for the recovery phase. This optimal control problem can be considered as two associated with the generation phase and recovery phase.

A. Generation Phase

During the generation phase, we need to maximize the traction force with minimum energy for thrust. Then the objective function can be written as below for the generation phase, F_t is traction force, $\dot{d}$ is the rate of distance, and η_2 is efficiency from electrical energy to motor to rotate the propeller. And from equation (9), we can derive the force represented in body frame. The traction force F_t is aligned with the tether line; therefore, we need to extract the radial direction component of the acceleration of a glider in the spherical frame.

$$J_G = \int_0^{t_{f1}} F_t \dot{d}\, dt - \int_0^{t_{f1}} \frac{TV}{\eta} dt \tag{20}$$

$$\begin{aligned} F^c &= \begin{bmatrix} T - D - W\sin\gamma + G_{xc} \\ W\cos\gamma\sin\phi + G_{yc} \\ -L + W\cos\gamma\cos\phi + G_{zc} \end{bmatrix} \\ F_t &= \begin{bmatrix} \sin\vartheta\cos\varphi & \sin\vartheta\sin\varphi & \cos\vartheta \end{bmatrix} C_{NC} F^c \\ \dot{d} &= \frac{x\frac{dx}{dt} + y\frac{dy}{dt} + z\frac{dz}{dt}}{d} \end{aligned} \tag{21}$$

where F^c is a force vector represented in body frame, $\dot{d}$ is the rate of the distance.For the propeller power, based on empirical operational data, we can simplify $\frac{TV}{\eta}$ as the function of thrust $P(T)$. Then, we can rewrite the objective function.

$$J_G = \int_0^{t_{f1}} F_t \dot{d}\, dt - \int_0^{t_{f1}} P(T) dt \tag{22}$$

States are $\{x, y, z, V, \gamma, \psi\}$, and control variables are angle of attack, bank angle, thrust, and tether reaction force. And C_L, C_D are the function of α. Therefore, in this phase, we need to maximize the energy from traction force and minimize the energy for the thrust. During this phase, $\dot{d}$ should be non-negative because the glider should pull the tether continuously and as we use different main wing configuration, aerodynamic coefficients and lift, drag force is calculated based on unfolded configuration data $C_{0u}, C_{L_\alpha u}, C_{D0u}, C_{D_\alpha 1u}, C_{D_\alpha 2u}$ and Wing area S_u.

$$\max_{\alpha, T, \phi, G} J_G \tag{23}$$

$$\text{subject to} \dot{x} = f(x, u) \tag{24}$$

$$\text{initial condition } x(0) = x_0 \tag{25}$$

$$d(0) = \sqrt{x(0)^2 + y(0)^2 + z(0)^2} \tag{26}$$

$$\text{terminal condition } d(t_f) = d_{t_f} = \sqrt{x(t_f)^2 + y(t_f)^2 + z(t_f)^2} \tag{27}$$

$$\text{control variable } 0 \le T \le T_{\max}, 0 < \phi \le \phi_{\max}, \alpha_{\min} \le \alpha \le \alpha_{\max}, G_{\min} \le G \le G_{\max} \tag{28}$$

$$\dot{d} > 0 \tag{29}$$

$$V_{min} \le V \le V_{max} \tag{30}$$

$$G_x = -G\sin\vartheta\cos\varphi,\ G_y = -G\sin\vartheta\sin\varphi,\ G_z = -G\cos\vartheta \tag{31}$$

$$C_L = C_{L0u} + C_{L_\alpha u}\alpha, C_D = C_{D0u} + C_{D_\alpha 1u}\alpha + C_{D_\alpha 2u}\alpha^2 \tag{32}$$

$$L = \tfrac{1}{2}\rho S_u V_r^2 C_L,\ D = \tfrac{1}{2}\rho S_u V_r^2 C_D \tag{33}$$

$$V_r = V - V_w \tag{34}$$

$$\dot{x} = V\cos\gamma\cos\psi + V_{wx},\ \dot{y} = V\cos\gamma\sin\psi + V_{wy},\ \dot{z} = -V\sin\gamma \tag{35}$$

$$\dot{V} = \tfrac{T-D+G_{xc}}{m} - g\sin\gamma \tag{36}$$

$$\dot{\gamma} = \tfrac{L\cos\phi - G_{yc}\sin\phi - G_{zc}\cos\phi}{mV} - \tfrac{g\cos\gamma}{V} \tag{37}$$

$$\dot{\psi} = \tfrac{L\sin\phi + G_{yc}\cos\phi - G_{zc}\sin\phi}{mV\cos\gamma} \tag{38}$$

$$P(T) = PT_0 + PT_1 \times T + PT_2 \times T^2 \tag{39}$$

B. Recovery Phase

When the glider needs to be recovered, the glider flies back to the initial point of the generation phase, the motor also takes back the tether line. In this phase, we need to minimize the energy consumption of both the glider and the motor. The glider changes to a folded configuration will benefit from reducing the resistance from wind and save time for recovery. We assume that the motor operates with constant power. The objective function is written as below;

$$J_R = -\int_{t_{f1}}^{t_{f2}} P_{\text{rw}}dt - \int_{t_{f1}}^{t_{f2}} P(T)dt \tag{40}$$

In a same manner, the folded wing configuration data ($C_{0f}, C_{L_\alpha f}, C_{D0f}, C_{D_\alpha 1f}, C_{D_\alpha 2f},$ and S_f) will apply to this problem to calculate aerodynamic forces. And power consumption of motor is constant $P_{\text{rw}} = 6$. Then, we can formulate the optimal control problem for the recovery phase. In this phase, the glider is not affected by the tether reaction force. The initial condition of this problem is the terminal condition of the generation phase problem.

$$\max_{C_L, T, \phi} J_R \tag{41}$$

$$\text{subject to } \dot{x} = f(x, u) \tag{42}$$

$$\text{terminal condition } x(t_{f2}) = x(0) \tag{43}$$

$$\text{control variable } 0 \le T \le T_{\max}, 0 < \phi \le \phi_{\max}, \alpha_{\min} \le \alpha \le \alpha_{\max} \tag{44}$$

$$t_{f2} \le t_{\max} \tag{45}$$

$$C_L = C_{L0f} + C_{L_\alpha f}\alpha, C_D = C_{D0f} + C_{D_\alpha 1f}\alpha + C_{D_\alpha 2f}\alpha^2 \tag{46}$$

$$L = \tfrac{1}{2}\rho S_f V_r^2 C_L,\ D = \tfrac{1}{2}\rho S_f V_r^2 C_D \tag{47}$$

$$V_r = V - V_w \tag{48}$$

$$\dot{x} = V\cos\gamma\cos\psi + V_{wx},\ \dot{y} = V\cos\gamma\sin\psi + V_{wy},\ \dot{z} = -V\sin\gamma \tag{49}$$

$$\dot{V} = \tfrac{T-D+G_{xc}}{m} - g\sin\gamma \tag{50}$$

$$\dot{\gamma} = \tfrac{L\cos\phi - G_{yc}\sin\phi - G_{zc}\cos\phi}{mV} - \tfrac{g\cos\gamma}{V} \tag{51}$$

$$\dot{\psi} = \tfrac{L\sin\phi + G_{yc}\cos\phi - G_{zc}\sin\phi}{mV\cos\gamma} \tag{52}$$

$$P(T) = PT_0 + PT_1 \times T + PT_2 \times T^2 \tag{53}$$

IV. Simulation

A. Integrated Model

To build the entire system of the AWES, we need to connect each virtual subsystem model. In this paper, we utilize Matlab Simulink to check its performance and validate the net gain of the entire production cycle's energy. Fig. 4 demonstrates how the entire system work and relation of each subsystem.

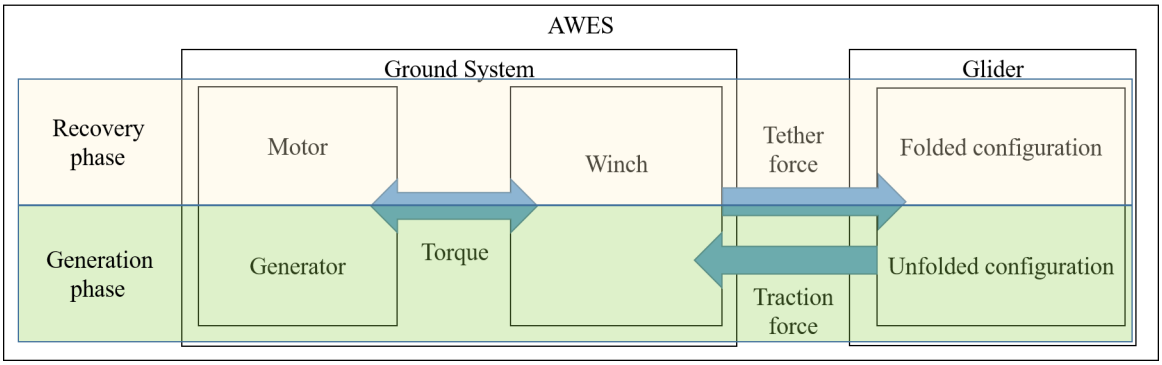

Fig. 4 The overview of the AWES model

During the Generation phase, the glider has an unfolded configuration, which is equivalent to general glider geometry. It provides traction force to the winch and winch to convert that force to rotational motion to the generator. For the recovery phase, glider changes to folded configuration fly back to the generation phase location, and the motor rewinds the tether.

Winch / DC machine specification	
radius $[m]$	0.03
mass [kg]	0.066
mass per unit length $[\mathrm{kg}/m]$	0.0004
back-emf constant $[V/rpm]$	0.013
total inertia $[\mathrm{kg}m^2]$	0.000192
viscous friction coefficient $[Nms]$	0.0002
coulomb friction torque $[Nm]$	0.11337

Table 1 Specification of winch and DC machine

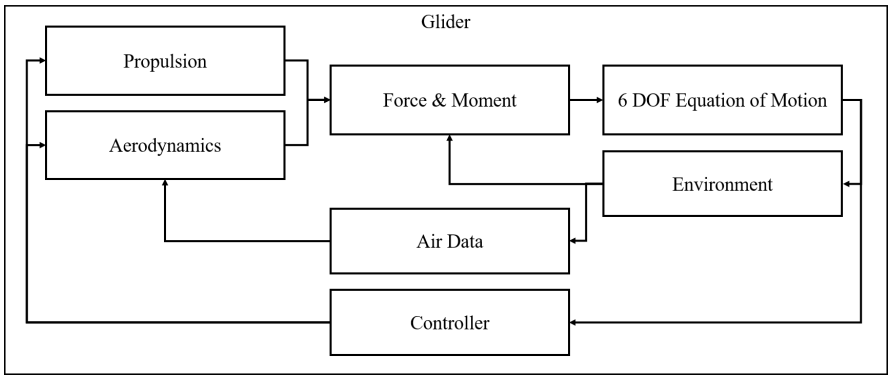

Fig. 5 The overview of a glider model

The glider model in this virtual simulation environment consists of several blocks, as shown in Fig. 5. 6 DOF equation of motion block built based on the dynamics of the glider, the environment block generates Gravitational Force, speed of sound, air density, speed of the wind, and Angular velocity of wind, based on the location and velocity of the glider. Air Data block calculates airspeed, angle of attack, and dynamic pressure. Combined with controllers output, Aerodynamic block generates aerodynamic coefficients. Force & Moment block sum all the external forces and moments to the glider. The glider has two configurations with the main wing, as shown in Fig. 6, we need to apply the parameters of each configuration, such as wingspan and moment of inertia, appropriately. In Table. 2, the glider's specification between both configurations are shown below;

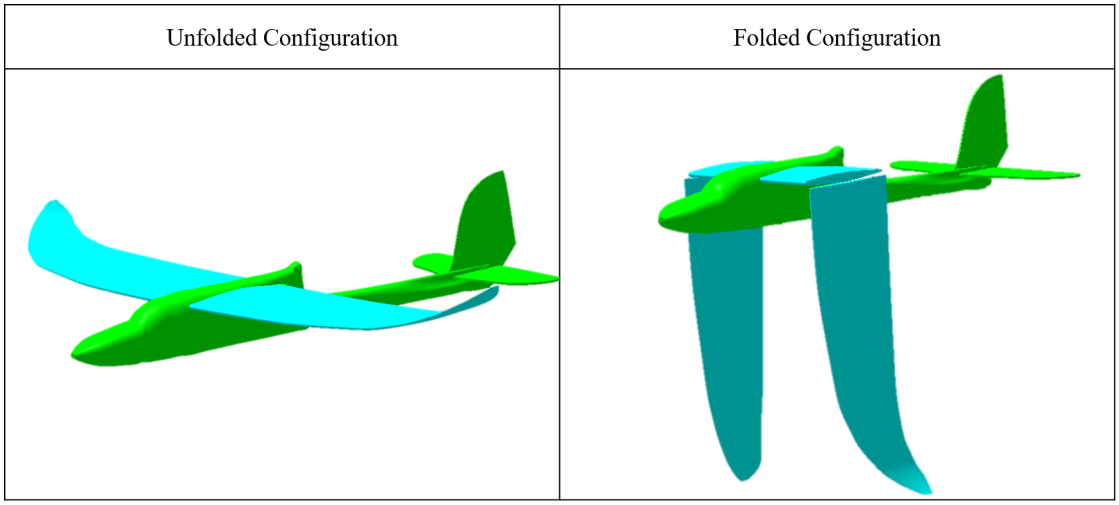

Fig. 6 Two configurations of a glider

Glider specification	
Wingspan $[m]$ (b_u/b_f)	1.1 / 0.22
Length $[m]$	0.867
Weight (incl. avionics) [kg]	0.738
Moment of inertia $[kgm^2]$ (I_{gu}/I_{gf})	$\begin{bmatrix} 0.0194 & 0 & -0.001454 \\ 0 & 0.01762 & 0 \\ -0.001454 & 0 & 0.03499 \end{bmatrix} / \begin{bmatrix} 0.009606 & 0 & -0.0007104 \\ 0 & 0.02077 & 0 \\ -0.0007104 & 0 & 0.02204 \end{bmatrix}$

Table 2 Glider Specification with unfold/fold configuration

B. Optimal Path

Combined with two problems, the optimal path will be calculated based on the condition below. The solution to this problem satisfies the criteria; the net gain of the energy should be positive, as shown in Fig. 7. Table 3 presents the result and constraints of this problem. The energy with negative sign means to gain energy. On the other hand, positive energy refers to consumption. In this case, we assume the wind blows from south to north.

Fig .8 presents states and control variable during a one cycle. And the result of a nominal glider and a foldable wing glider will be presented in the final manuscript.

V. Conclusion

This paper demonstrates the new concept of the aerial vehicle with a foldable wing with improved energy efficiency. First, we build a glider and a DC machine to emulate their mechanical and electrical characteristics. We formulate an optimal control problem with different dynamics and constraints as a multi-phase optimal control problem. A folded

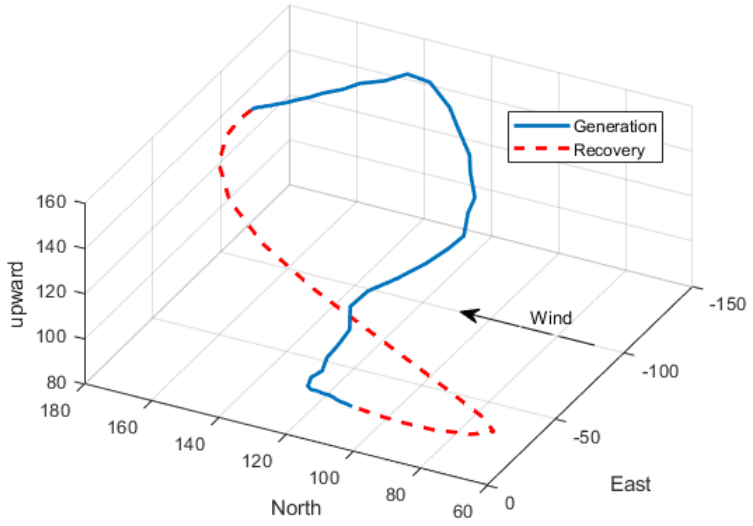

Fig. 7 A glider trajectory of one cycle

Result		Constraints	
Overall energy gain $[J]$	-862	Wind Speed $[m, \text{direction}]$	3m/s South
Generation energy $[J]$	-2048	distance, d_{tf} $[m]$	250
Energy for thrust $[J]$	1121	glider velocity, V $[m]$	$5 \leq V \leq 25$
Energy for rewinding $[J]$	63.81	angle of attack, α[rad]	$-0.35 \leq \alpha \leq 0.35$
Period of generation phase $[s]$	14.24	bank angle [rad]	$-1 \leq \phi \leq 1$
Period of recovery phase $[s]$	10.70	Thrust, T [N]	$0 \leq T \leq 8$

Table 3 Optimal control problem results and constraints

configuration benefits from reduced wind resistance during the recovery phase, the result of the changed geometry of the glider provides reduced power consumption. Lastly, the comparative simulation results validate the enhanced efficiency of the new concept. Future research will explore the operation of the physical AWES system in outdoor environments. The proposed can be applied to larger-scale with extended cycle period AWES that has a higher traction force and improved efficiency of the generator.

References

[1] Statistics, G. W., "Global wind energy council," *Washington, DC, USA*, 2017.

[2] Loyd, M. L., "Crosswind kite power (for large-scale wind power production)," *Journal of energy*, Vol. 4, No. 3, 1980, pp. 106–111.

[3] Cherubini, A., Papini, A., Vertechy, R., and Fontana, M., "Airborne Wind Energy Systems: A review of the technologies," *Renewable and Sustainable Energy Reviews*, Vol. 51, 2015, pp. 1461–1476.

[4] Lunney, E., Ban, M., Duic, N., and Foley, A., "A state-of-the-art review and feasibility analysis of high altitude wind power in Northern Ireland," *Renewable and Sustainable Energy Reviews*, Vol. 68, 2017, pp. 899–911.

[5] Jehle, C., and Schmehl, R., "Applied tracking control for kite power systems," *Journal of Guidance, Control, and Dynamics*, Vol. 37, No. 4, 2014, pp. 1211–1222.

[6] Williams, P., Lansdorp, B., and Ockesl, W., "Optimal crosswind towing and power generation with tethered kites," *Journal of guidance, control, and dynamics*, Vol. 31, No. 1, 2008, pp. 81–93.

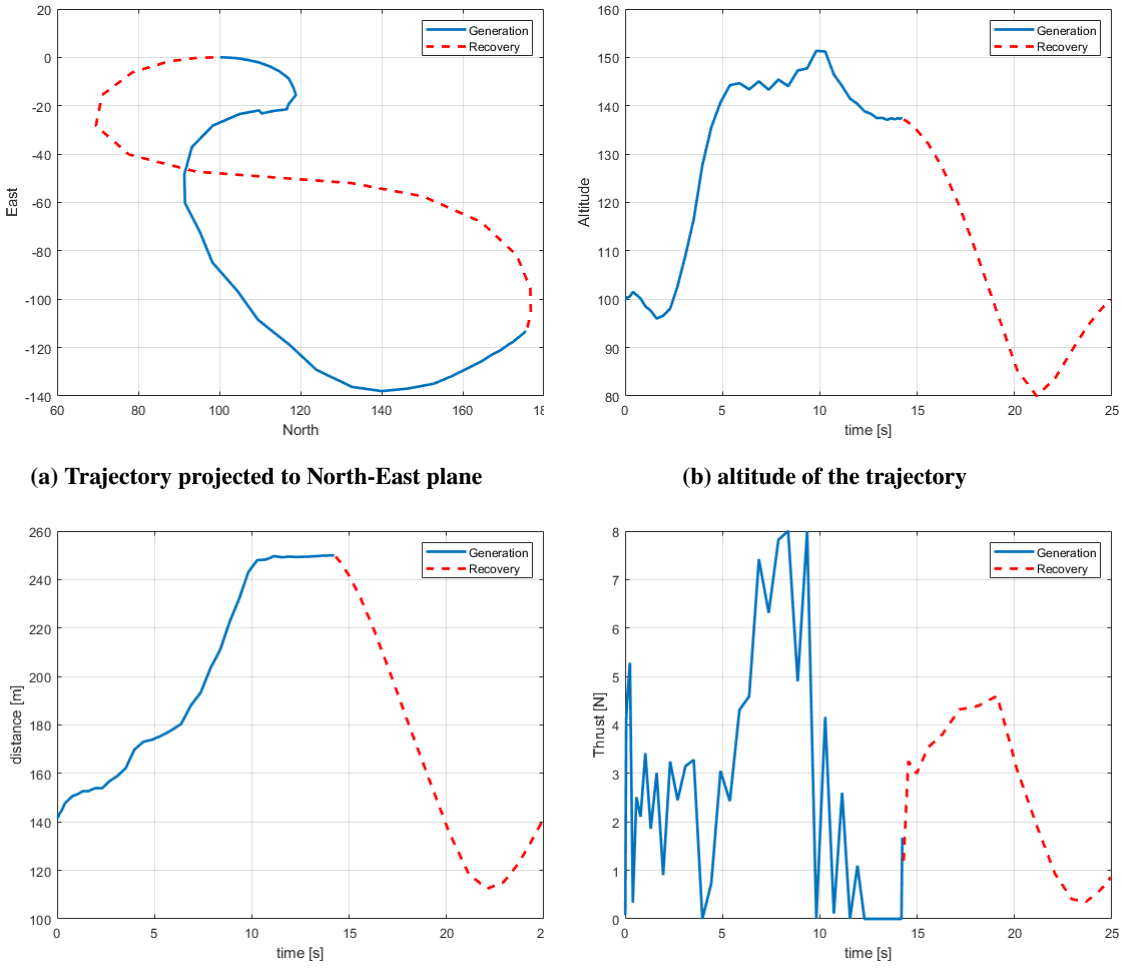

(a) Trajectory projected to North-East plane

(b) altitude of the trajectory

(c) Distance of the trajectory

(d) Thrust of a glider

Fig. 8 Time histories of the cycle

[7] Canale, M., Fagiano, L., and Milanese, M., "KiteGen: A revolution in wind energy generation," *Energy*, Vol. 34, No. 3, 2009, pp. 355–361.

[8] Bormann, A., Ranneberg, M., Kövesdi, P., Gebhardt, C., and Skutnik, S., "Development of a three-line ground-actuated airborne wind energy converter," *Airborne wind energy*, Springer, 2013, pp. 427–436.

[9] Fagiano, L., Zgraggen, A. U., Morari, M., and Khammash, M., "Automatic crosswind flight of tethered wings for airborne wind energy: Modeling, control design, and experimental results," *IEEE Transactions on Control Systems Technology*, Vol. 22, No. 4, 2013, pp. 1433–1447.

[10] Krenciszek, J., Akindeinde, S. O., Braun, H., Marcel, C., Okyere, E., and Argatov, I., "Mathematical modeling of the pumping kite wind generator: Optimization of the power output," *URL: http://www. win. tue. nl/casa/meetings/special/ecmi08/pumpingkite. pdf*, 2008.

[11] Terink, E., Breukels, J., Schmehl, R., and Ockels, W., "Flight dynamics and stability of a tethered inflatable kiteplane," *Journal of Aircraft*, Vol. 48, No. 2, 2011, pp. 503–513.

[12] Rautakorpi, P., "Mathematical modeling of kite generators," Master's thesis, 2013.

[13] Milutinović, M., Kranjčević, N., and Deur, J., "Multi-mass dynamic model of a variable-length tether used in a high altitude wind energy system," *Energy conversion and management*, Vol. 87, 2014, pp. 1141–1150.

[14] Williams, P., Lansdorp, B., and Ockels, W., "Modeling and control of a kite on a variable length flexible inelastic tether," *AIAA Modeling and Simulation Technologies Conference and Exhibit*, 2007, p. 6705.

[15] Li, H., Olinger, D. J., and Demetriou, M. A., "Attitude tracking control of a groundgen airborne wind energy system," *2016 American Control Conference (ACC)*, IEEE, 2016, pp. 4095–4100.

[16] Li, H., Olinger, D. J., and Demetriou, M. A., "Attitude tracking control of an airborne wind energy system," *Airborne Wind Energy*, Springer, 2018, pp. 215–239.

[17] Ruiterkamp, R., and Sieberling, S., "Description and preliminary test results of a six degrees of freedom rigid wing pumping system," *Airborne wind energy*, Springer, 2013, pp. 443–458.

[18] Canale, M., Fagiano, L., Ippolito, M., and Milanese, M., "Control of tethered airfoils for a new class of wind energy generator," *Proceedings of the 45th IEEE Conference on Decision and Control*, IEEE, 2006, pp. 4020–4026.

[19] Weitz, L. A., "Derivation of a point-mass aircraft model used for fast-time simulation," *MITRE Corporation*, 2015.